

SCIENTIFIC OBJECTIVES AND DESIGN CONCEPT OF THE SPECTROMETERS FOR PROPOSED FLYBY MISSION TO MAIN BELT COMET 133P/ELST-PIZARRO. Hao Zhang¹, Bicen Li², Jianjie Yin², Weigang Wang², Jiangchuan Huang³, and Chih-Hao Hsia⁴. ¹China University of Geosciences, Wuhan, China (zhanghao@cug.edu.cn); ²Beijing Institute of Space Mechanics and Electronics, China Academy of Space Technology, Beijing, China; ³Beijing Institute of Spacecraft System Engineering, China Academy of Space Technology, Beijing, China; ⁴Macau University of Science and Technology, Macau, China.

Introduction: The discoveries of main belt comets (MBCs) (e.g., [1][2]) in early twentieth century have triggered great interest of the planetary society as these volatile rich bodies are located in the main belt and thus may have played a key role in supplying water to the early Earth. Therefore, MBCs are interesting and important candidate objects for space missions [3][4]. Here we first summarize the scientific objectives of the optical and infrared spectrometers for a proposed flyby mission to 133P/Elst-Pizarro. Then we present the observational data of visible, near-infrared, thermal infrared spectra and phase curves that are currently available. Finally we describe the design concept for the spectrometers based on the known optical and thermal properties of the target.

Scientific objectives: (1) Determine the compositions and production rates of volatiles (H_2O , CO_2 , NH_3 , CH_4 , H_2S , and others); (2) Search for and characterize organic materials (C_2H_6 , CH_3OH , H_2CO , HCN etc.); (3) Determine the size distributions and production rate of dust particles; (4) Characterize the mineralogy, geology and surface structures of the body; (5) Understand the triggering mechanisms of activities and characterize any subsurface materials exposed; (6) Determine the diurnal and orbital activities that controlled by both the body's geometric properties and thermal environment; (7) Compare the results with other missions to asteroids and comets to understand the formation and evolution of the MBCs.

Observational data: The visible [5] and near-infrared [6] reflectance spectra of 133P/E-P are shown in Fig.1 (a). As 133P/E-P appears to be B or F type, the spectra of (419) Aurelia and (704) Interamnia (from Small Body Node) are also shown for comparisons. The thermal infrared spectra measured by WISE [7] and Spitzer with NEATM fitting to Spitzer are shown in Fig. 1(b). The disk-integrated phase curves (R-filter) for 133P/E-P [8] and the C-type (253) Mathilde [9] (with diameter and distances taken into account and converted to radiance factors), as shown in Fig.2, are fitted by Hapke's integral brightness function with 5 parameters (single scattering albedo, shadow hiding opposition parameters B_{s0} and h , two-term Henyey-Greenstein phase function parameters b and c , with a fixed roughness of 20°) [10]. These observational data and model fittings

can be used to constrain the surface materials and payload development.

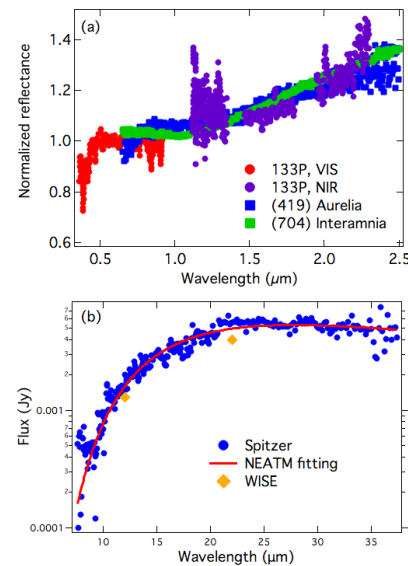


Fig. 1. (a)Visible and near-infrared reflectance spectra of 133P/E-P [5][6] and two F bodies, (419) Aurelia and (704) Interamnia, (b) WISE [7] and Spitzer measured thermal infrared spectra of 133P/E-P with NEATM fitting to Spitzer.

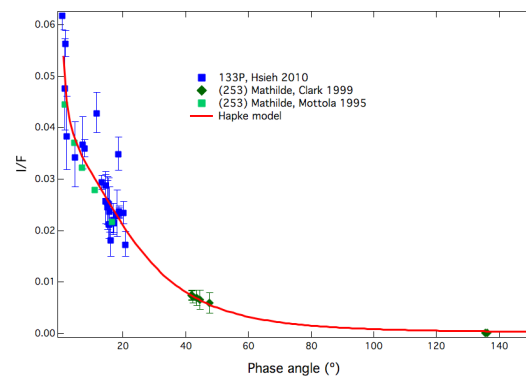


Fig. 2. Phase curve of 133P/E-P and that of C-type (253) Mathilde with 5-parameter Hapke model fitting. All phase curve data in absolute magnitude have been converted to radiance factor.

Design concept: Our proposed spectral coverage is from 0.4 to $50 \mu m$ by using two spectrometers covering $0.4\sim 5 \mu m$ [11] and $5.7\sim 50 \mu m$ [12], respectively. The visible and near infrared imaging spectrometer (VIIS)

consists of a Shafer telescope and an Offner spectrometer (Fig. 3) covering 0.4 to 5 μm with a spectral resolution of 5 nm in the visible and 10 nm in the near infrared, respectively. The spatial resolution of the VIIS is 0.5 m at an observing distance of 5 km. The compactness of the VIIS is achieved by dispersing both visible and near-infrared light beams through the same grating substrate with different densities of grooves (Fig. 4). The signal to noise ratio of the VIIS is better than 100 using cryogenic optics technology.

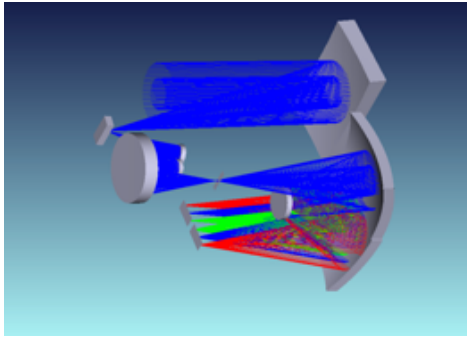


Fig. 3. Optical system of visible and near-infrared imaging spectrometer.

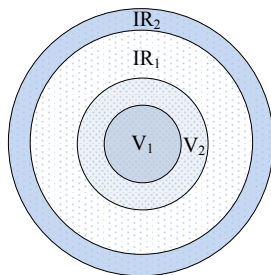


Fig. 4. Grating configuration of the VIIS.

The mid- and far-infrared spectra will be measured by a thermal emission spectrometer (TES) with a wavelength coverage of 5.7–50 μm [12]. To meet the requirements of wide spectral coverage, high spectral resolution (8 cm^{-1}) and high signal-to-noise ratio, a Ritchey-Chretien optical system (Fig. 5), a time modulation Fourier transform spectrometer and uncooled pyroelectric detector are employed. The major components of the TES are shown in Fig. 6. The key component is an interferometer (Fig. 7) with two corner cubes and swing arms. The spatial resolution of TES is 10 m at an observing distance of 5 km. The TES uses a pyroelectric detector working at ambient temperature and the signal to noise ratio of the spectrometer is better than 320 from 5.7 to 35 μm .

Summary: The prototype instruments are under development and will be tested in simulated space environment.

Extensive work on their calibrations, characterizations and measurements on analog materials will be carried out.

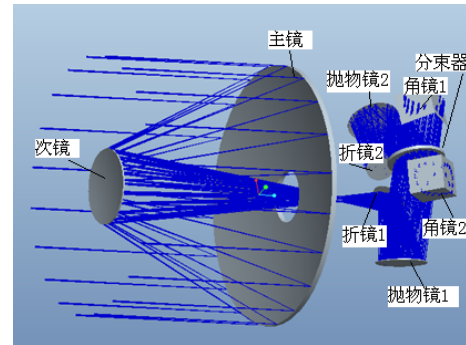


Fig. 5. Optical system of the thermal emission spectrometer.

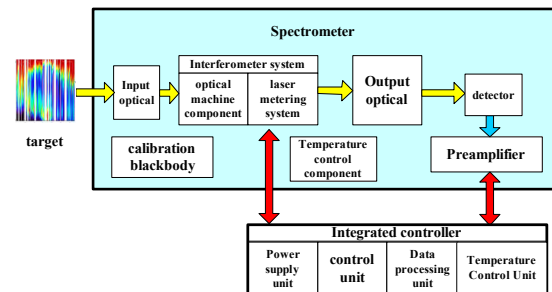


Fig. 6. Major components of the thermal emission spectrometer.

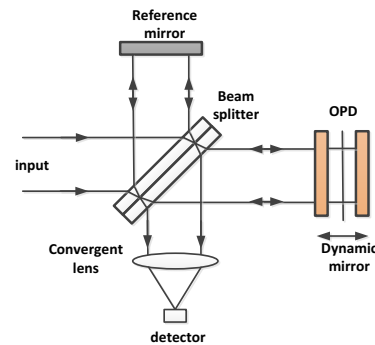


Fig. 7. The interferogram is generated by the Michelson interferometer in every two seconds.

References: [1] Jewitt D. et al. (2004) *AJ*, 127, 2997-3017. [2] Hsieh H. et al. (2009) *ApJ*, 694, L111-L114. [3] Snodgrass C. et al. (2017) *Adv. Space Res.*, 62, 1947-1976. [4] Jones G. H. et al. (2018) *Adv. Space Res.*, 62, 1921-1946. [5] Licandro J. et al. (2011) *A&A*, 532, A65. [6] Rousselot P. et al. (2011) *Icarus*, 211, 553-558. [7] Bauer J. M. et al. (2012) *ApJ*, 747, 49. [8] Hsieh H. et al. (2010) *MNRAS*, 403, 363-377. [9] Clark B. E. et al. (1999) *Icarus*, 140, 53-65. [10] Hapke B. (1984) *Icarus*, 59, 41-59. [11] Coradini A. et al. (1998) *PSS*, 46, 1291-1304. [12] Christensen P. R. et al. (2016) *Space Sci. Rev.*, 214, 87.